Articles

NMR Structural Studies of the Supramolecular Adducts between a Liver Cytosolic Bile Acid Binding Protein and Gadolinium(III)-Chelates Bearing Bile Acids Residues: Molecular Determinants of the Binding of a Hepatospecific Magnetic Resonance Imaging Contrast Agent

Michael Assfalg,[†] Eliana Gianolio,[‡] Serena Zanzoni,[†] Simona Tomaselli,[§] Vito Lo Russo,[||] Claudia Cabella,[⊥] Laura Ragona,[§] Silvio Aime,*[,‡] and Henriette Molinari*[,†]

Dipartimento Scientifico e Tecnologico, Università di Verona, Strada Le Grazie 15, 37134 Verona, Italy, Dipartimento di Chimica, Università di Torino, Via Pietro Giuria 7, Torino, Italy, ISMAC-CNR, Via Bassini 15, 20133 Milano, Italy, Bracco Imaging SpA, via E. Folli 50, 20134 Milano, Italy, and Bracco Imaging Spa, via Ribes 5, 10010 Colleretto Giacosa (TO), Italy

Received April 4, 2007

The binding affinities of a selected series of Gd(III) chelates bearing bile acid residues, potential hepatospecific MRI contrast agents, to a liver cytosolic bile acid transporter, have been determined through relaxivity measurements. The Ln(III) complexes of compound **1** were selected for further NMR structural analysis aimed at assessing the molecular determinants of binding. A number of NMR experiments have been carried out on the bile acid-like adduct, using both diamagnetic Y(III) and paramagnetic Gd(III) complexes, bound to a liver bile acid binding protein. The identified protein "hot spots" defined a single binding site located at the protein portal region. The presented findings will serve in a medicinal chemistry approach for the design of hepatocytes-selective gadolinium chelates for liver malignancies detection.

Introduction

Bile acid synthesis from cholesterol is the primary pathway for cholesterol catabolism.[1] Bile acids are amphipathic molecules that contain a sterol scaffold with hydroxyl groups and a side chain that terminates in a carboxyl group. Their amphipathic nature is essential to solubilize dietary lipids, which subsequently promotes their absorption in the digestive tract. Most of the bile acids are present within the enterohepatic organs. They are usually stored in the gallbladder, however, when a meal is ingested, they flow into the duodenum and intestine. Bile acids are efficiently (95%) absorbed again by passive diffusion and active transport in the ileum and transported back to the liver via the portal vein. In the liver, they are taken up at the basolateral membrane and exported again at the apical membrane of the hepatocytes into the bile canaliculus, thus completing their enterohepatic circulation.[2,3] Besides their roles in dietary lipid absorption and cholesterol homeostasis, it has become clear that bile acids are also signaling molecules.[4]

In the bile acids enterohepatic circulation, three key steps are mediated by (i) a receptor system that binds bile salts on one surface and translocates them into the cell; (ii) a cellular bile salt binding protein that moves them across the cell; and (iii) an exit system, which moves bile salts out of the other side of the cell.[5] Within this framework bile acid binding proteins (BABPs[a]) were proposed to act as the putative bile acid carriers in the cytosol.[6−8] BABPs, belonging to the fatty acid-binding protein (FABP) family, are small molecular mass proteins (14−15 kDa) exhibiting the typical fold of the family in which 10 strands of antiparallel β-sheet surround the hydrophobic ligand binding cavity and two short α-helices are located between the first and the second strands. We have recently reported the NMR structural characterization of chicken liver bile acid binding protein (cL-BABP) in complex with two identical bile salts,[9] and the acquired knowledge on binding mode has prompted us to investigate, in the present paper, a novel type of interaction between a model BABP protein, from chicken liver, and different conjugates in which a Gd(III) complex is linked to a bile acid through a spacer.[10] The rationale for the design of such conjugates derived from a search for new hepatospecific MRI contrast agents in which a lipophilic residue was linked to the basic unit of diethylenetriaminepentaacetic acid (DTPA). These "lipophilic complexes" enter hepatocytes by means of active transport mechanism mediated by organic anion transport polypeptides (OATP). Interestingly, it was shown that OATPs are not expressed in the basolateral membrane of some hepatoma cell lines, thus making these systems diagnostic of specific hepatic malignancies.[10,11] Indeed, it has been recently reported that the low molecular weight gadolinium chelate, with laboratory code B22956/1 and with proposed international nonproprietary name gadocoletic acid trisodium salt[12] (Gd-2 in this work), is a new contrast agent showing high biliary excretion, which could be potentially advantageous in hepatobiliary imaging. It is in fact a good substrate to the liver specific OATP1B3, reported to be poorly expressed or absent in human liver tumors.[13] Gd-2 is known to enter hepatocytes, from where it is excreted into the bile to an extent depending on the animal species. As preliminary pharmacokinetic studies in healthy

* To whom correspondence should be addressed. Phone: +39 0116707520 (S.A.); +39 0458027901 (H.M.). Fax: +39 0116707855 (S.A.); +39 0458027929 (H.M.). E-mail: silvio.aime@unito.it (S.A.); molinari@sci.univr.it (H.M.).

[†] Università di Verona.

[‡] Università di Torino.

[§] ISMAC-CNR.

[||] Bracco Imaging Spa, Milano, Italy.

[⊥] Bracco Imaging Spa, Colleretto Giacosa (TO), Italy.

[a] Abbreviations: DTPA, diethylenetriaminepentaacetic acid; BABP, bile acid binding protein; STD, saturation transfer difference; HSQC, heteronuclear single quantum coherence; GCDA, glycochenodeoxycholic acid.

10.1021/jm070397i CCC: $37.00
Published on Web 10/04/2007

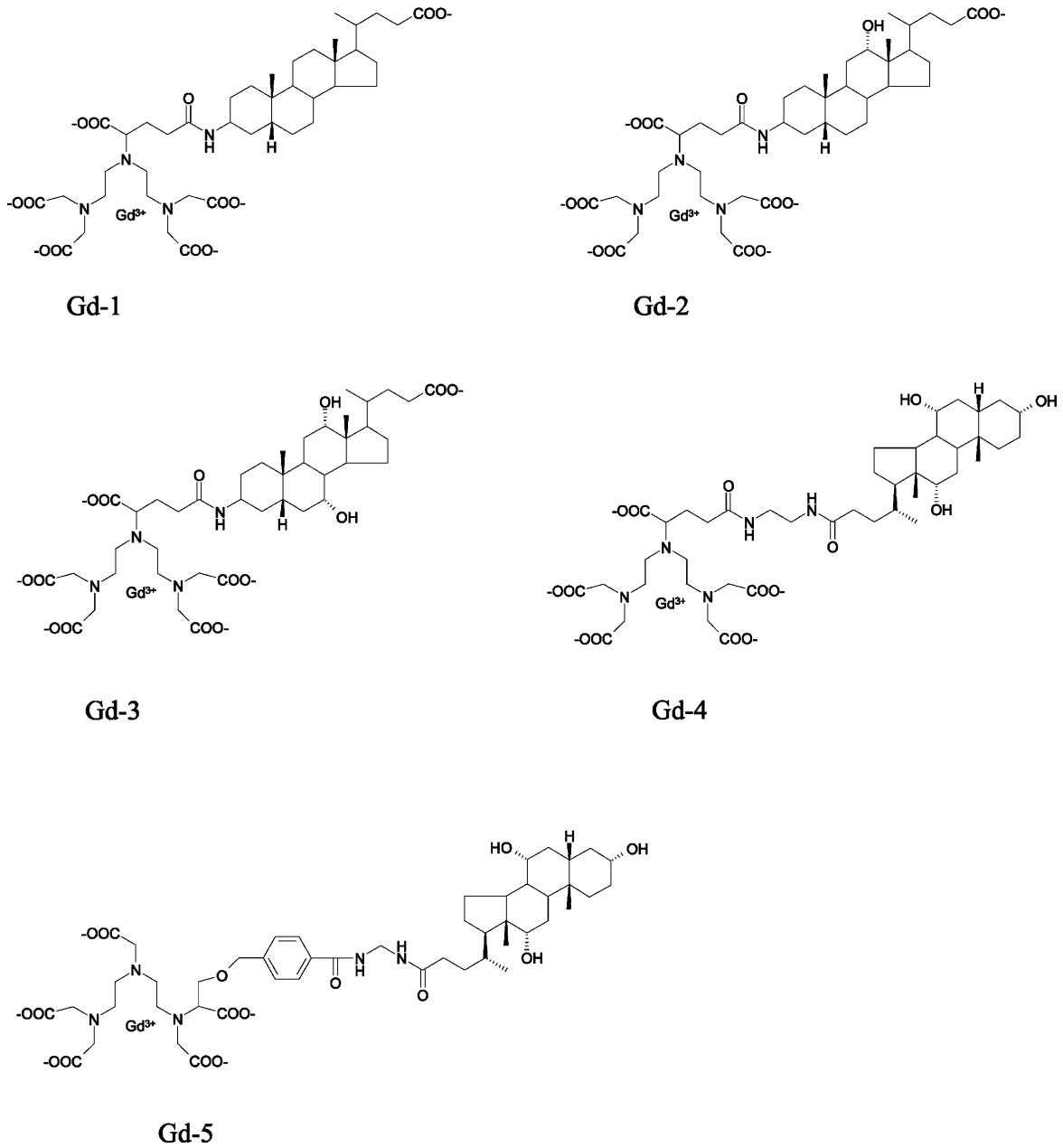

Figure 1. Structure of the Gd(III)−DTPA−bile acid conjugates under investigation in the present paper.

volunteers have shown that the biliary excretion is the primary route of elimination, the study of the mechanism involved in the transport of bile acid-like diagnostic agents within hepatocytes is crucial to understand the molecular determinants of such circulation.[14] In this line, it is clear that the structural features of the adduct of Gd(III)/bile acid conjugates with the liver cytosolic carrier protein is an important step toward the design of liver-selective contrast agents. Such a design is highly needed as, up to now, the only hepatocyte-selective contrast agent that has been approved for clinical use is mangafodipir trisodium Mn-DPDP (Manganese(II) *N*,*N*′-dipyridoxylethylenediamine-*N*,*N*′-diacetate-5,5′-bisphosphate), whereas gadolinium diethylenetriaminepentaacetic acid (Gd−DTPA) and gadolinium ethoxybenzyl diethylenetriaminepentaacetic acid (Gd−EOB−DTPA) are contrast agents that are both hepatocytes-selective and show extracellular distribution.[15]

In the present paper, a relaxivity study is presented, aimed at the screening of the affinity constants and relaxivity properties of a series of Gd(III)/bile acid chelate/cL-BABP adducts, followed by a detailed NMR study of the "best" complex, namely, Gd-1, exhibiting the highest affinity toward the protein and belonging to the so-called "second-generation conjugates".[10] At first, a wide variety of NMR experiments have been performed on the diamagnetic Y(III) analogue of Gd-1, called Y-1, easily amenable to structural studies. Interaction data have been subsequently completed with the NMR analysis of the corresponding Gd(III) derivative. The ensemble of the structural data clearly defines the stoichiometry, the affinity, and the protein binding site for this novel complex and opens the way to a detailed analysis of the molecular factors governing the interactions of these conjugates within the framework of enterohepatic circulation.

Results and Discussion

Relaxometric Analysis of the Complex between Gd(III)/Bile Acid Conjugates and cL-BABP. A series of Gd(III)-DTPA/bile acid conjugates have been tested for their binding capability with cL-BABP. The analyzed Gd complexes, shown

Table 1. Dissociation Constants (K_d) and Relaxivity (r_{1p}^b) Measured for Different Gd(III)−DTPA/Bile Acids Bound to cL-BABP[a]

Gd complex	r_{1p} (mM^{-1} s^{-1})	K_d (M^{-1})	r_{1p}^b (mM^{-1} s^{-1})
Gd-1	8.4 ± 0.15	$5.88 \pm 1.34\ 10^{-6}$	24.3 ± 0.26
Gd-4	7.0 ± 0.12	$1.72 \pm 0.395\ 10^{-5}$	18.4 ± 0.34
Gd-5	6.8 ± 0.10	$3.75 \pm 0.760\ 10^{-5}$	20.3 ± 0.55
Gd-2	8.6 ± 0.14	$2.12 \pm 0.270\ 10^{-4}$	23.4 ± 0.95
Gd-3	8.5 ± 0.13	$1.94 \pm 0.245\ 10^{-3}$	24.0 ± 0.23

[a] Relaxivity values (r_{1p}) measured for the unbound Gd(III)−DTPA/bile acids are reported for comparison.

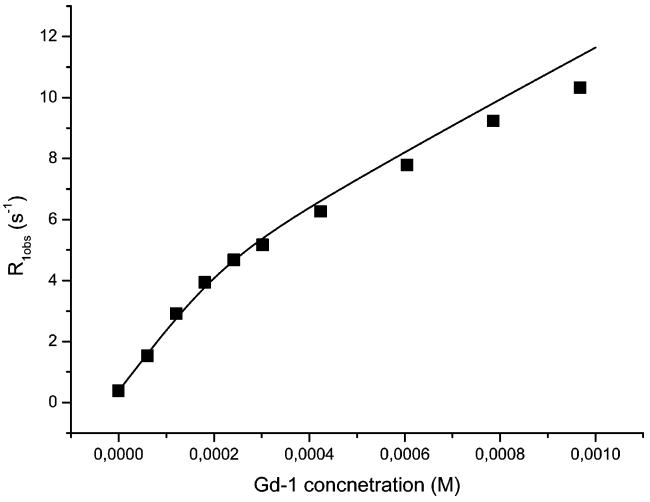

Figure 2. Plot of the water proton relaxation rate of a 0.13 mM solution of cL-BABP as a function of the Gd-1 concentration (0.47 T, 25 °C, neutral pH).

in Figure 1, belong to a group of conjugates, previously selected and described,[10,16] differing by (i) the nature of bile acid, (ii) the site of conjugation of the Gd(III) complex to the bile acid moiety, and (iii) the global charge of the conjugate. For each Gd complex, the water relaxivity (defined as the relaxation enhancement of water protons in the presence of the paramagnetic complex at 1 mM concentration) was determined; the obtained values are reported in Table 1. The evaluation of the binding parameters to cL-BABP was obtained with the relaxometric approach called proton relaxation enhancement (PRE), which exploits the increase in relaxation rate of the paramagnetic complex determined by its binding to a macromolecular substrate.[17]

Two different types of experiments were carried out: in the first, the enhancement of the water proton relaxation rate of a Gd complex solution was measured in the presence of increasing amounts of cL-BABP, to determine the dissociation constant (K_d) and the relaxivity value (r_{1p}^b) of the adduct (Table 1 and Supporting Information). In the second, a fixed concentration of cL-BABP was titrated with the Gd complex to determine the number of specific binding sites (n; Figure 2).

In general, it appears that the conjugation of bile acids to the Gd(III)−DTPA complex reduces their affinity to the protein, given that K_d values smaller than 10^{-6} M have been reported for the chenodeoxycholic acid.[9] For all the selected compounds, a 1:1 protein/ligand stoichiometry was found, differently from the 1:2 protein/ligand stoichiometry reported for BABPs from different species in complex with bile acids.[6,8] By inspection of Table 1, a clear relationship between the affinity constants and the structural features of the compounds can be inferred. For example, Gd-1, Gd-2, and Gd-3 differ by the number of hydroxyl groups present on the steroid rings, and the measured K_d values increase by 1 order of magnitude for each hydroxyl group added to the steroid (Table 1). It appears that a decreased hydrophobicity and/or an increase in steric hindrance of the bile acid in the complex determine a lower affinity. Furthermore, when considering the same bile acid, the K_d is much lower for the complexes conjugated at position C^{24} (Gd-5, Gd-4) than for those bearing the conjugation at C^3 (Gd-3). This observation is in agreement with the recently solved NMR (PDB ID 2JN3) and X-ray (PDB ID 1TW4) structures of cL-BABP in complex with chenodeoxycholate and cholate molecules, respectively. In these structures, it is clear that the preferred orientation of the steroid moieties is the one with the carboxylate tail protruding toward the solvent and the C^3 unit buried within the protein cavity. Indeed, it is expected that functionalization at C^3 forces the bile acid derivative to assume a different orientation with respect to that observed in the natural bile acid−transporter protein adduct. On the other way it should be kept in mind that many factors enter in the evaluation of the efficacy of potential contrast agents, such as pharmacokinetic evaluations. The analyzed derivatives were previously classified as first-, second-, or third-generation conjugates depending upon the site of conjugation of the Gd(III) chelate to the bile acid and on the presence of coupling of the bile acid carboxylic moiety to a functionalized α-amino acid. It was observed that several second-generation conjugates, where the Gd(III) complex is linked to position C^3 of the steroid moiety, showed high biliary elimination as well as good tolerabilities.[10] These observations, together with the higher affinity displayed by Gd-1 toward cL-BABP, made it the compound of choice for further detailed NMR structural analysis.

The determination of the binding stoichiometry of the Gd complexes to cL-BABP was obtained through a titration experiment monitored by relaxometry analysis, where the protein concentration was kept fixed, and that of the Gd complex was increased stepwise. The titration data for Gd-1 complex are displayed in Figure 2 as an example. In the first part of the titration, the total concentration of the Gd complex is much lower than that of the protein, and the Gd complex can be considered almost completely bound. Here the increase in relaxivity depends on n, K_d, and r_{1p}^b (where n is the number of binding sites and r_{1p}^b is the relaxivity of the complex bound to the protein). In the second part of the titration, the total Gd-complex concentration is much higher than that of the protein, therefore, the protein is almost completely bound and the slope of the curve depends on the free Gd-complex concentration. The number of binding sites can be estimated from the value of the protein−ligand molar ratio at which the change in the slope of the titration curve occurs. In the present case, this ratio was equal to one, because the protein concentration used for the experiment was 0.13 mM and the change in slope occurred at a ligand concentration of about 0.14 mM. The relaxivity values of the supramolecular adducts with cL-BABP are very similar for all the investigated complexes, being 21.3 ± 3 mM^{-1} s^{-1} at 20 MHz and 25 °C, that is, about three times the corresponding values for the free complexes.

The relaxometric properties for the Gd-1-(cL-BABP) adduct were investigated in detail recording the $1/T_1$ NMRD (nuclear magnetic relaxation dispersion) profiles at 25 °C and 37 °C (Figure 3). The analysis of the experimental data in paramagnetic complexes is usually performed using the Solomon−Bløm-bergen−Morgan theory, which is not valid for slowly rotating systems when the electronic levels are split at zero field. For this reason, the fitting was obtained using a modified theory[18,19] that takes into account the static zero field splitting effects. In

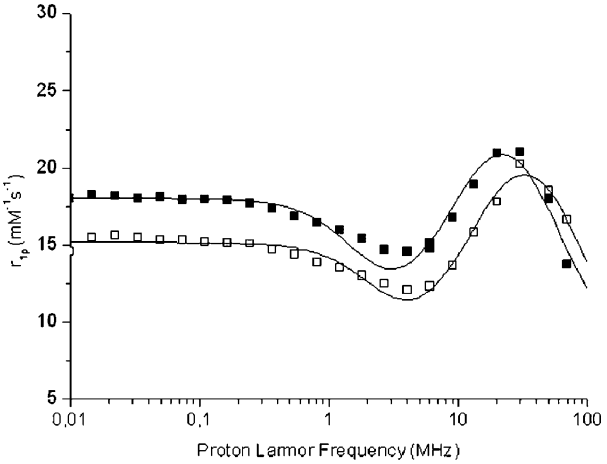

Figure 3. Nuclear magnetic resonance dispersion profiles of Gd-1 at 25 °C (filled square) and 37 °C (empty squares), normalized to 1 mM concentration of Gd(III) ion. The solid curves through the data points were calculated using the Solomon−Bloembergen equations according to the Lipari−Szabo approach. The value of q (number of coordinated water molecules) was assumed to be 1; the distance between Gd(III) ion and the protons of the coordinated water molecule was fixed at 3.1 Å, while the distance between Gd(III) ion and the outer sphere water proton nuclei at 3.8 Å; the solute−solvent diffusion coefficient was fixed at 2.24 × 10−5^5 cm^2 s^{-1}. Exchange lifetime (τ_M) was fixed to the value obtained from ^{17}O NMR studies on the free Gd complex (137 ns, data not shown).

addition, the equations were modified according to Lipari−Szabo approach. This model allows determining the presence of local mobility, with an associated short correlation time τ_l, on top of a slower global motion with an associated correlation time τ_g. The global correlation time associated with the adduct Gd-1/cL-BABP was assumed to be equal to the protein τ_g measured by high-resolution NMR[6] (7.1 ns at 25 °C) and was fixed to that value during the fitting procedure. At 25 °C, the obtained τ_l value was 504 ps. By increasing the temperature to 37 °C, these values decreased to 431 ps and 5.2 ns for τ_l and τ_g, respectively. In both cases, the general order parameter ($0 < S^2 < 1$) describing the degree of spatial restriction of the local motion has been found to be very low (0.15), suggesting a substantial freedom of motion of the Gd complex bound to the protein. The overall decrease of the molecular reorientational rates is responsible for the high-field shift of the relaxivity peak observed in the $1/T_1$ NMRD profile at 37 °C as compared to the one recorded at 25 °C. Interestingly, the relaxivity maxima at the two temperatures is the same (though shifted by ca. 10 MHz), suggesting that the attained relaxivities are not quenched by the occurrence of a not fast enough exchange of the coordinated water molecule as often reported for supramolecular adducts between albumin and Gd(III) complexes.[20,21] In the herein considered system, the detection of a relatively low relaxivity value can be ascribed essentially to the occurrence of a local motion of the Gd(III) chelate around the spacer that links the paramagnetic moiety and the recognition synthon.

Cellular Uptake Measurements. Given the promising data already described in the introduction about the differential cellular uptake of Gd-2, similar experiments were repeated with Gd-1 to assess whether this important feature is maintained by this compound. In Figure 4, the quantities of Gd-1, Gd-2, and Gd(III)−DTPA internalized into rat hepatocytes and hepatomes (HTC) in the presence of the Gd(III) complexes in the incubation medium are reported. The above quantities were determined by measuring the relaxation rates (20 MHz) of the cytosolic extracts once all the Gd(III) complexes have been mineralized

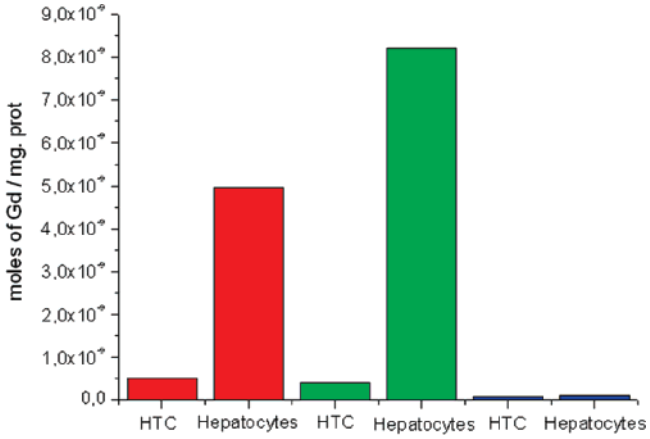

Figure 4. Comparison of cellular uptakes of Gd-1 (green), Gd-2, and (red) Gd(III)−DTPA (blue) on hepatocytes (as model of healthy cells) and HTC (as model of tumor cells) performed at 37 °C for 6 h.

to Gd(III) aquo-ion (see Experimental Section). Cells have been incubated at 37 °C for 6 h with a concentration of Gd complex in the culture medium of 0.25 mM. Likely, Gd(III)−DTPA enters the cells only by pynocitosis and therefore the low amounts detected in hepatocytes and in HTC just reflect the limited pynocitotic activity of these cells. The uptake of Gd-1 and Gd-2 by HTC is only slightly higher than that shown by Gd−DTPA, whereas the same complexes are internalized to a much larger extent into hepatocytes. Indeed, the differential uptake of Gd-2 and Gd-1 between the healthy and the tumoral cells is 10 and 20 times, respectively. Finally, the better performance of Gd-1 in respect to Gd-2 is consistent with its enhanced binding to cL-BABP.

NMR Experiments on Gd-1 in the Metal-Free and Metal-Bound Forms. Compound **1** contains a steroid skeleton that gives rise to a very crowded proton NMR spectrum (Figure 5A). Indeed, most resonances fall in the narrow 1−2.5 ppm region, called the "hump" region, and are split in multiplets because of scalar couplings. At the magnetic field used for the measurements (500 MHz), second-order effects further complicate the interpretation of the spectra. Nevertheless, with the aid of a combination of 1D and 2D spectra, including COSY, TOCSY, NOESY, and *J*-resolved experiments, we could perform the assignments of all proton resonances of compound **1**. A good entry point for the assignment of the steroidal skeleton was given by the low-field resonating amide H^{25} proton (for proton numbering, see Scheme 1), which displayed well-resolved scalar connectivities to protons of the first cyclohexane ring (Figure 6). On the other hand, the presence of an intense methyl doublet signal attributable to H^{21} and displaying connectivities with the contiguous aliphatic chain allowed drawing structural connectivities on the opposite side of the steroid moiety. The assignment reported in the literature for 5β-cholanoic acid also proved useful at various stages of the assignment procedure.[22] The remaining signals were assigned in the following way. A spin system made by four resonances was identified in the TOCSY spectrum (Figure 6, top panel). The detailed analysis of the coupling patterns and of the multiplet structure allowed us to assign it to the protons attached to C^{27}, C^{28}, and C^{29}, with the two H^{27} resonances being degenerate. Another spin system constituted by four proton signals at 2.92, 3.12, 3.22, and 3.4 ppm was assigned to the two $C^{32}H_2$−$C^{33}H_2$ branches (Figure 6, top panel). Finally, the four $C^{35}H_2$ methylene groups appeared as degenerate signals resonating at 3.8 ppm.

For most high-resolution NMR analyses, a diamagnetic analog of Gd-1 was used, where the bound metal ion was Y(III) in

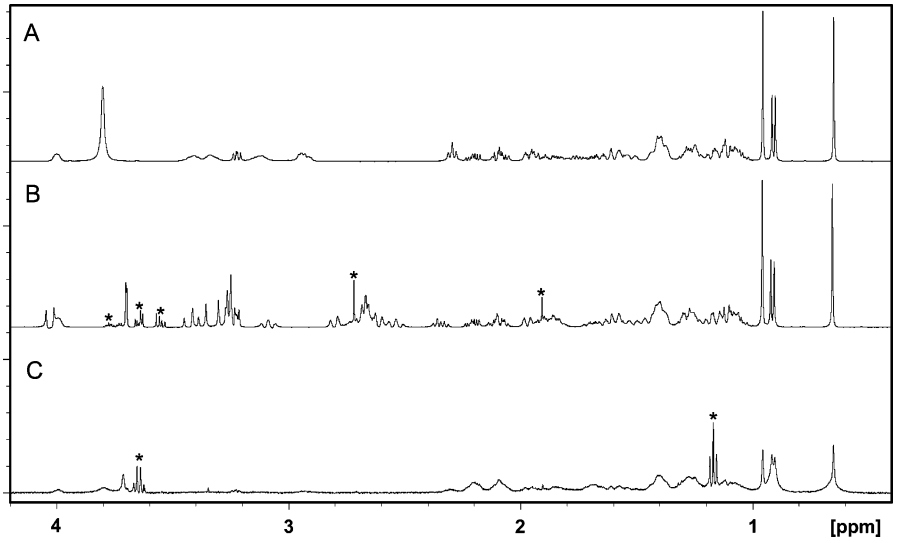

Figure 5. ^{1}H NMR (500 MHz, 1D) spectra of ligand 1 (A), Y-1 (B), and Gd-1 (C) acquired on 1 mM samples in 30 mM phosphate buffer, pH 7, 90% H_2O/10% D_2O, at 25 °C. Major sample impurities are marked by asterisks.

Scheme 1

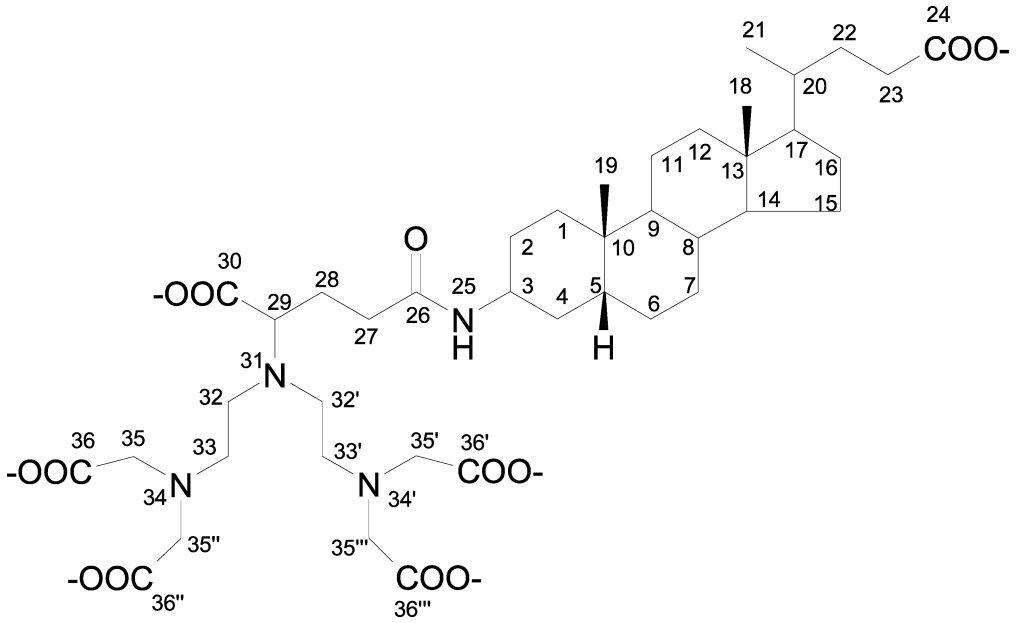

place of Gd(III). The 1D proton NMR profile of Y-1 (Figure 5B) appears quite different from that of the metal-free compound because of the metal coordination and the consequent structural rearrangement of the DTPA moiety. The resonances of the high field region of the spectrum are barely affected by the coordination, thus suggesting that the steroid part of the molecule behaves independently from the metal-chelating group. In the spectral region comprised between 2 and 4 ppm, major signal changes are observed. In particular, it appears that the degeneracy of the $C^{35}H_2$ methylene protons is removed. The TOCSY scalar connectivities and the *J* coupling values were used for the assignment. Geminal coupling constants are measurable with precision from the *J*-resolved spectrum (Figure 7). A spin system of five resonances comprised between 1.9 and 3.2 ppm was assigned to the linker protons (attached to carbons C^{27} to C^{29}), while a four-resonance spin pattern in the region 2.5 to 3.2 ppm was attributed to protons of the $C^{32}-C^{33}$ groups (Figure 6, bottom panel).

The NMR spectrum of Gd-1 shows a reduced number of peaks, as compared to that of the Y(III) complex, and significant line broadening is evident (Figure 5C). Gadolinium ion is strongly paramagnetic because of the presence of seven unpaired electrons. The high spin multiplicity is maintained also after complexation by common chelating agents, and the spherical symmetry of the 4*f* orbitals explains the absence of chemical shift effects on the signals of nearby nuclei. However, unpaired electrons affect markedly the nuclear relaxation of neighboring nuclei through the pseudo-contact mechanism, producing an increase in the NMR line widths. The extent of paramagnetic-induced line broadening depends on the distance between the observed nucleus and the paramagnetic ion. Thus, all signals from the DTPA group and the linker atoms are broadened beyond detection, as they are in very close proximity to the paramagnetic center. The remaining signals, belonging to protons that are farther apart, are still visible but have increased line widths.

Identification of the Interacting Epitope of Diamagnetic Y-1 with cL-BABP. The nuclear spin transverse relaxation rate, R_2, is a commonly used probe of binding due to its nearly direct dependence on the overall molecular rotational correlation time.

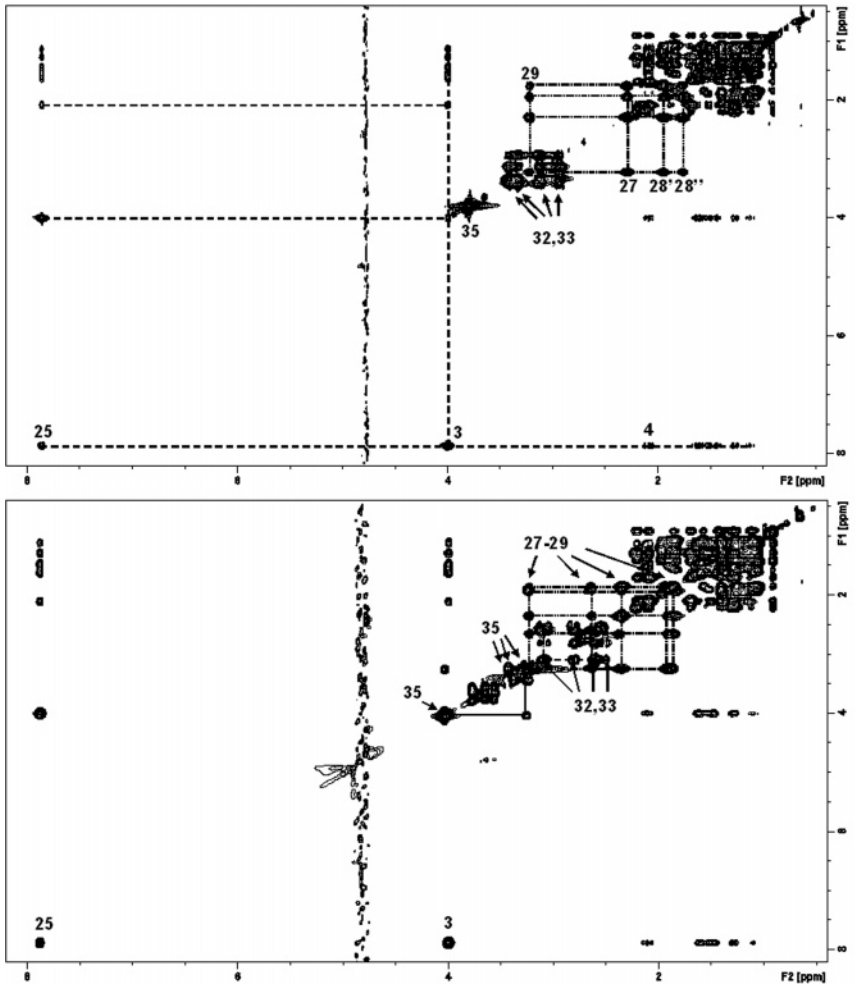

Figure 6. Proton 2D-TOCSY spectra of ligand 1 (top panel) and of Y-1 (bottom panel). The spectra were registered at 500 MHz on a 1 mM sample in 30 mM phosphate buffer, pH 7, 90% H_2O/10% D_2O, at 25 °C. Numbering indicated on cross-peaks corresponds to protons indicated in Scheme 1.

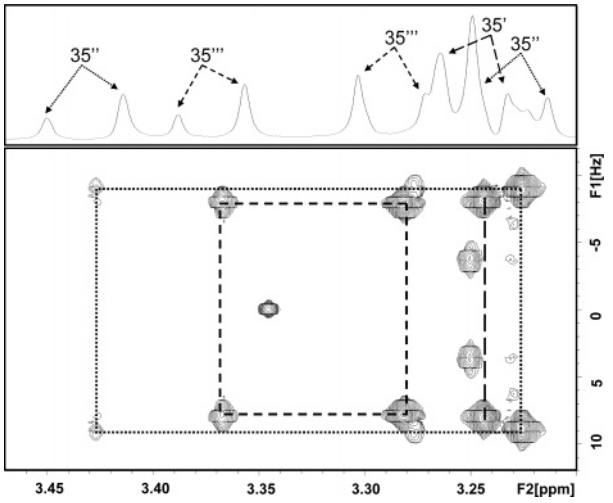

Figure 7. Aliphatic region of the 1D ^1H spectrum of Y-1 displaying five of the six assigned doublet resonances of $C^{35}H_2$ methylene resonances (top panel); region of the proton 2D-*J*-resolved NMR spectrum showing the same doublets (bottom panel).

Ligands that undergo sufficiently rapid exchange will possess exchange-averaged relaxation rates that reflect exchange-mediated transfer of R_2^{bound} to the free state. An exchange contribution R_{ex} due to the nonequivalence of free versus bound chemical shifts may further add to binding-induced relaxation rate enhancement. The amplitude of the transverse relaxation rate affects the line width (R_2/π) and the signal intensity ($\propto R_2^{-1}$). Under certain experimental conditions, even a small amount of an interacting protein may determine line broadening of the ligand resonances. Indeed, by addition of cL-BABP to a 1 mM solution of Y-1 at a molar ratio of 1:30, selected signals display an increase in the line width. Among these are the resonances of the bile acid moiety of the complex and of the linker atoms. No line broadening is observed for the signals of the DTPA moiety. These data indicate that the bile acid moiety is directly involved in binding, while the metal ion chelating part of the compound retains a certain degree of freedom in the bound form.

The above observations are rather qualitative and provide no information about which atoms of Y-1 are directly interacting with cL-BABP. To get more detailed information about binding, we have undertaken saturation transfer difference (STD) measurements. These experiments rely on the possibility to saturate all protein resonances after selective irradiation of certain protein signals and propagation of the saturation to all nuclei via the mechanism of spin diffusion.[23] In the presence of a ligand, the saturation is transferred to the interacting compound which can persist in its saturated state also after dissociation. By performing the difference between two spectra registered with on- and off-resonance irradiation, only the signals of interacting ligand atoms are observed, allowing for the so-called epitope mapping. Using the same sample employed for the line-broadening experiment, the STD spectrum displayed in Figure 8 was obtained. The spectrum shows the presence of the signals assigned to the

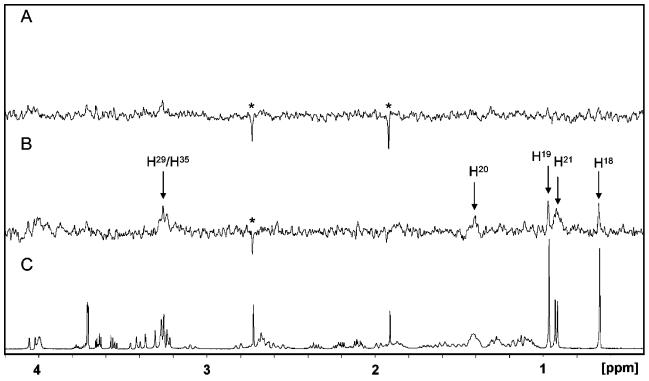

Figure 8. STD experiment performed on a sample of Y-1 alone (A) and in the presence of cL-BABP 30:1 (B). For comparison, the 1D spectrum of the compound is displayed in (C).

methyl groups and to H^{20}. Another signal appears in correspondence of the resonating frequency of H^{29} and one H^{35}, but because of this ambiguity, this weak signal was not further considered. As all the resonances assigned in the STD spectrum correspond to atoms that mostly belong to the steroid moiety, the latter probably constitutes the binding epitope, although the involvement of further atoms in the interaction with the protein cannot be ruled out. Indeed, STD peaks may have escaped detection because of the low sensitivity of the present experiment which was hampered by unfavorable experimental conditions: the small molecular weight and high mobility of the protein prevented efficient spin-diffusion, and the broad spectral window of the ligand resonances made it impossible to use stronger saturating conditions without directly irradiating the ligand nuclei.

NMR Titration of Y-1 into ^{15}N-Labeled cL-BABP. The interaction of cL-BABP with Y-1 was here investigated by titrating the unlabeled compound into ^{15}N-labeled protein and recording a series of ^{1}H−^{15}N-heteronuclear single quantum coherence (HSQC) spectra. These experiments have become very popular in protein−ligand interaction studies,[24] including drug-screening, because chemical shifts are very sensitive indicators of binding events and their changes can be immediately translated into structural information once the resonance assignments are known. The assignment of the resonances in each spectrum was made starting from those available from the literature for apo-cL-BABP[6,25] and transferring them by visual comparison of successive titration steps, where possible. Confirmation of the assignments was obtained by analysis of the sequential correlations found in 3D HBHA(CO)NH and HNCA experiments registered at 500 and 900 MHz, respectively, for a protein/ligand ratio of 1:4. Of the 112 known assignments of the apoprotein, 98 could be followed, without ambiguity, during the titration. Inspection of the series of spectra shows that different behaviors are displayed by different peaks, namely, (1) no changes, (2) chemical shift changes with little or no intensity attenuation, and (3) chemical shift changes accompanied by significant line broadening. Figure 9 shows a superposition of the HSQC maps recorded at protein/ligand ratios 1:0, 1:2, and 1:5, highlighting signals representative of the above classes. It appears that only a restricted number of peaks remains unaffected by addition of the Y(III)−DTPA/bile-acid conjugate, indicating that the protein undergoes significant conformational changes upon binding. The presence of a large number of peaks that are shifted and attenuated during the titration can be explained by the occurrence of a conformational exchange equilibrium between the protein in the apo and holo forms at a rate that is intermediate on the chemical shift time

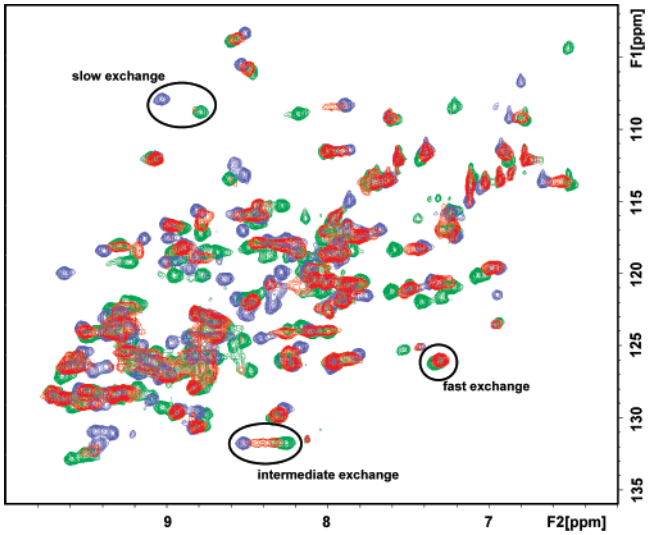

Figure 9. Superposition of the ^{1}H−^{15}N HSQC maps recorded at three different protein (P)/ligand (L) molar ratios; P/L 1:0 (green), 1:1 (red), and 1:5 (blue).

scale. At the same time, some signals may be affected by the direct interaction of the corresponding amino acid residues with the ligand. The deconvolution of the two simultaneously occurring events is not trivial, and the chemical shift mapping approach cannot be rigorously applied to identify the binding site. However, some signals appear to be more influenced by one event or the other. It can be noted, for example, that some amide cross-peaks, all defining a unique region (10, 15, 23, 26, 27, 29, 34), undergo very little intensity attenuation, thus reflecting chemical exchange processes that are relatively fast on the NMR time scale. It is reasonable to conclude that the position change of these peaks is determined only by ligand binding and not by conformational rearrangement. By mapping the residues corresponding to such peaks onto the protein structure, it appears that they are mostly located in the helix−loop−helix region. The chemical shift titration data were fitted assuming a simple one-site binding, in agreement with relaxivity data, to estimate the dissociation constant, and representative fitted curves are displayed in Figure 10. K_d values in the range of 5 to 150 μM were obtained, with an average value of 66 μM, thereby confirming the affinity of Gd-1 for cL-BABP determined from relaxometric measurements.

Identification of the Protein Binding Site from Paramagnetic Relaxation and Competition Experiments. When highly paramagnetic gadolinium ions get close to proton nuclei, the NMR signals of the latters are severely broadened. In a tight protein/gadolinium-complex adduct, the dominant correlation time for the paramagnetic-induced nuclear relaxation rate enhancement is the long electronic relaxation time or the rotational correlation time of the adduct, and NMR analysis of the nuclei surrounding the unpaired electrons is made impossible. In the case of weaker interactions between the diamagnetic protein and the paramagnetic ligand, more favorable conditions can be encountered when the exchange rate becomes the dominant mechanism to modulate the electron−nucleus dipolar interaction. The signal-disrupting effect of paramagnetism can also be attenuated if an excess of protein over the gadolinium complex is used. We collected ^{1}H−^{15}N-HSQC spectra of the labeled protein in the presence of Gd-1 at a protein−ligand ratio of 1:0.05 and 1:0.1. Intensity attenuations determined from the spectra registered on the cL-BABP/Y-1 adduct were subtracted from those of the cL-BABP/Gd-1 spectra at the corresponding protein−ligand ratios, to extract the pure paramagnetic effect.

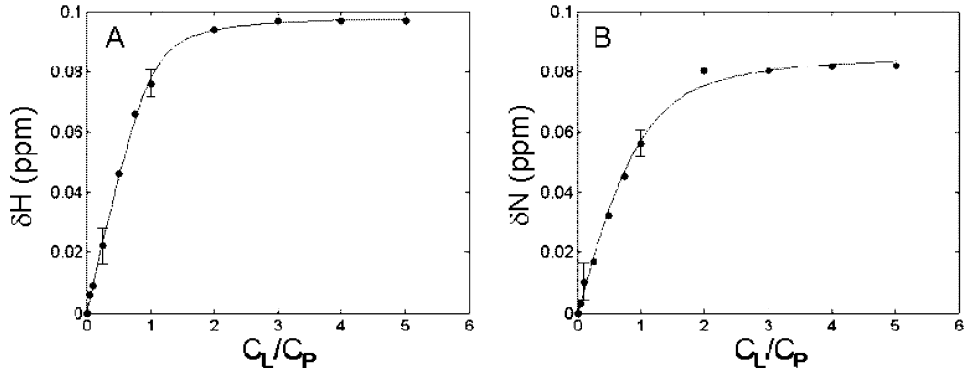

Figure 10. Example of ligand titration profiles for the interaction of Y-1 with cL-BABP. The plot shows (A) the proton amide chemical shift change δH_N for residue **29** and (B) the nitrogen amide chemical shift change δN_H for residue **15**, versus the total ligand to total protein (C_L/C_P) concentration ratio. The continuous curves were calculated by a fitting procedure, assuming a simple one-site binding (eq 1 in Experimental Section). The evaluated K_d values for the shown residues are 22 and 75 μM, respectively. Data were recorded at pH 7.2 and 25 °C. The error bars on selected points reflect the standard deviation from a mean of three measurements.

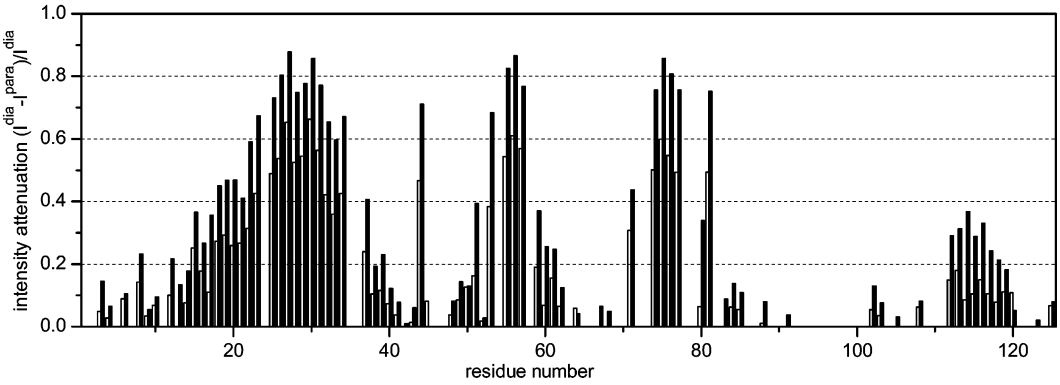

Figure 11. Histogram reporting the differential attenuation upon Gd-1 addition, evaluated at a protein/total ligand ratio of 1:5 with cL-BABP/Y-1/Gd-1 molar ratios of 1:4.76:0.24 (open bars) and 1:4.55:0.45 (filled bars) versus residue number. I^{para} is the intensity measured on each BABP/Y-1/Gd-1 sample. I^{dia} is the intensity measured on a BABP/Y-1 sample at the same specified protein/ligand ratio. Residues **24**, **36**, and **54** are prolines. Residues **69**, **70**, **72**, **73**, **78**, **79**, **82**, **86**, **89**, **92**−**101**, **109**−**111**, and **121**, though not unambiguously assigned, did not show intensity attenuations larger than 30%.

Attenuations larger than 50% are observed for residues **19**, **26**−**30**, **53**, and **56**, located mostly in helix II and loop CD, while also residues **20**−**23**, **25**, **31**−**33**, **51**, and **76** (the latter in loop EF) are attenuated by more than 30%. These data indicate that the so-called "portal region" located at the open end of the protein[6] constitutes the unique first interaction binding site to the apoprotein. Analogous experiments were run using mixed ligands in saturating conditions, that is, with a protein/total ligand ratio of 1:5, but with different relative amounts of the diamagnetic and the paramagnetic complexes. The two samples analyzed with HSQC experiments contained BABP/Y-1/Gd-1 in molar ratios of 1:4.76:0.24 and 1:4.55:0.45. The measurement of the intensities with respect to the sample containing only BABP and Y-1, that is, the diamagnetic reference, revealed that also in saturating conditions the same regions described above as being affected by the paramagnetic ion show strongly attenuated peaks. Indeed, attenuations larger than 50% were found for residues **26**, **27**, **29**−**31**, **55**−**57**, **74**−**76** (1:4.76:0.24 sample) and for residues **22**−**34**, **53**, **55**−**57**, and **74**−**77** (1:4.55:0.45 sample), as shown in Figure 11. The most perturbed residues observed with the 1:4.76:0.24 sample are mapped on the protein structure in Figure 12, panel A, while residues directly involved in the interaction with the Y-1 derivative are mapped in panel B.

By comparison of the data in nonsaturating and saturating conditions, it can therefore be inferred that the portal region is not only the first binding site but also the only one displayed by the protein for the analyzed compound. The spatial position of the most attenuated residues confirms the already described hypothesis, derived from the line-width analysis, that the Gd−DTPA moiety of the ligand remains outside the protein.

To investigate whether the binding site of Gd-1 overlaps with that of glycochenodeoxycholic acid (GCDA), a competition experiment was run. An HSQC spectrum was registered on a sample containing unlabeled cL-BABP and ^{15}N-labeled GCDA at a 1:0.3 ratio. The spectrum showed two distinct cross-peaks corresponding to GCDA bound to two different protein sites, indicated as 1 and 2 in Figure 13A,B, as previously observed.[9] The peak of the unbound ligand (normally found at 7.89 (^{1}H)−120.3 (^{15}N) ppm)[9] was not observable because the relative concentrations used for the experiment and the high affinity favored the formation of the adduct. Earlier studies showed that the upfield (proton frequency) peak 2 corresponds to the ligand bound to the more internal site, and the lowfield peak 1 to the more superficial site.[9] After addition of Y-1 in 5-fold excess with respect to the protein, the acquired HSQC spectrum still displayed the two cross-peaks in the same positions as before, but with strongly reduced intensities. On the other hand, a strong signal (peak 3) appeared 0.18 ppm upfield from peak 2 in the proton dimension (Figure 13C,D). The intensity of this peak corresponds to 86.0% of total intensity of all three peaks, with peaks 1 and 2 contributing 6.2% and 7.8%. When considering the relative intensities of peaks 1 and 2 before addition of Y-1 (49.0% and 51.0% of the total), it appears that their intensities were reduced by 42.7% and 43.2%, respectively, thereby showing that practically all the lost intensity (86.0%) was

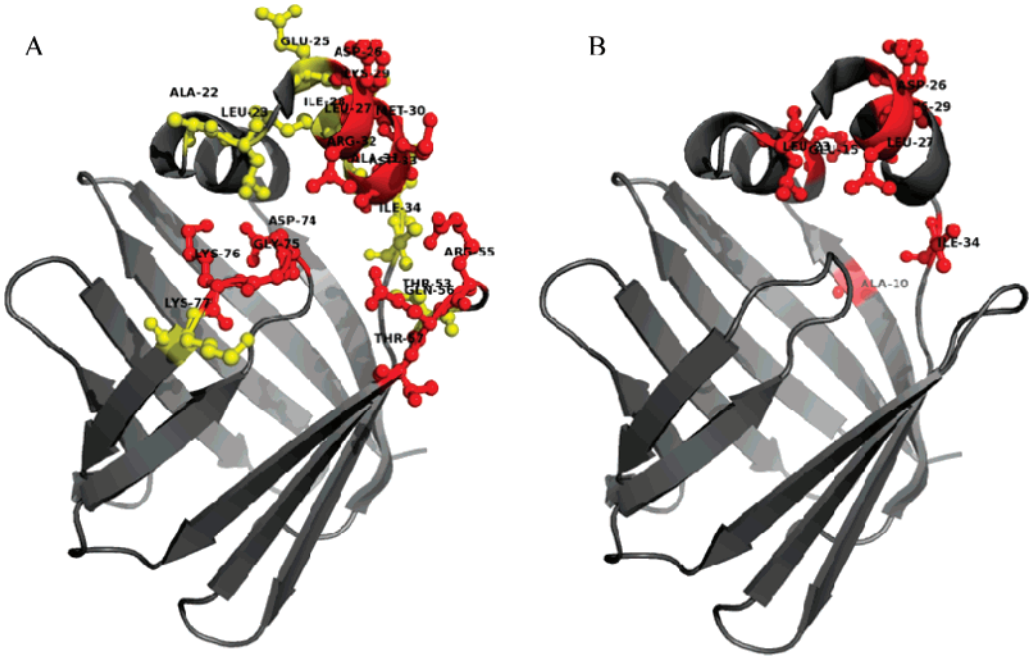

Figure 12. cL-BABP residues affected by binding to Gd-1 (cL-BABP/Y-1/Gd-1 molar ratios 1:4.76:0.24) are highlighted by a color code: attenuations larger than 30% (yellow) and larger than 50% (red; panel A); cL-BABP residues directly affected by binding to Y-1 (cL-BABP/Y-1 molar ratio 1:5) are depicted in red (panel B).

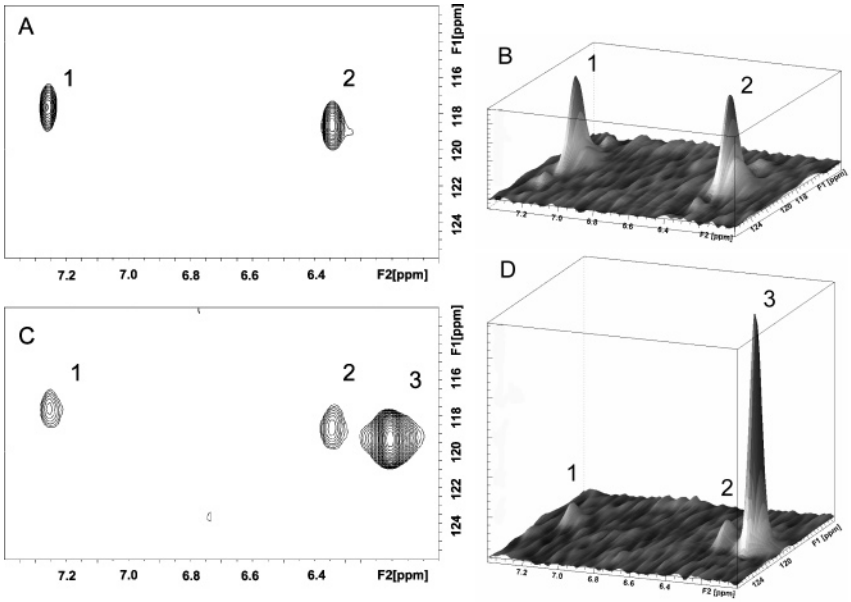

Figure 13. (A) 2D $^{1}H-^{15}N$ HSQC spectrum recorded at 500 MHz, 25 °C, and pH 7.2 (contour plot) of a sample containing a 1:0.3 mole ratio of unlabeled cL-BABP (0.4 mM) to ^{15}N GCDA. The resonances corresponding to the bile acid bound to sites 1 and 2 are designated 1 and 2, respectively; (B) a stacked plot representation of the spectrum shown in (A); (C) the spectrum of (A) after addition of 1:5 P/L molar ratio of unlabeled Y-1. The observed binding site for ^{15}N-GCDA, in the presence of the new ligand, is designated as 3; and (D) a stacked plot representation of the spectrum shown in (C).

transferred to peak 3. These data may be interpreted as follows: (i) Y-1 and GDCA are exclusive competitor binders to the portal region of cL-BABP; (ii) when Y-1 is bound, then only one further GCDA molecule can be bound to the internal site, the latter being slightly perturbed from its original structure and thus giving rise to a shift change for the ligand amide signal; and (iii) the affinity of Y-1 is lower than that of GCDA for the external site, thus although GCDA is present at lower concentration, a small fraction of protein molecules bound to two GCDA molecules are still detectable. The smaller line width of peak 3 (23.6 Hz), compared to that of peaks 1 (27.3 Hz) and 2 (27.4 Hz), might be related to the presence of a single GCDA molecule within the cavity, thus canceling out the chemical exchange between the two binding sites, which has been observed for a bile salt/cL-BABP complex by ROESY and NMR diffusion experiments (Eliseo, T., personal communication).

Conclusion

The primary aim of this study was the identification of the essential features of the interaction and the location of the binding site in a selected supramolecular adduct between a bile acid-like containing species, Gd-1, a potential hepatospecific

MRI contrast agent, and cL-BABP, a liver cytosolic transporter. The reported findings, derived from a wide variety of NMR experiments, confirm, on one side, the unique potential of NMR in tailoring simple experiments to investigate molecular recognition and, on the other side, add a new biological dimension to the design of liver specific contrast agents. Thus, the knowledge of the main features of the interaction with the carrier protein in the hepatic cytosol have now been acquired and added to the elucidation of the hepatocyte uptake of these systems by the membrane organic transporter anion proteins (OATPs). The identified "hot spots" of the interaction will guide the NMR structure determination of the complex, which represents a necessary step to guide the rational design of hepatocytes-selective gadolinium chelates for liver targeting.

Experimental Section

Protein Expression and Purification. Recombinant cL-BABP was expressed as soluble protein in *Escherichia coli* cells, purified with anion exchange and size-exclusion chromatography, and finally delipidated following already described protocols.[6] ^{15}N and ^{13}C isotope labeling was achieved using M9 minimal media containing 1 g/L $^{15}NH_4Cl$ and 4 g/L ^{13}C enriched glucose.

Conjugates Synthesis. All the analyzed conjugates were prepared as previously described[10,16] and kindly supplied by Bracco Imaging Spa (Milan).

Water Proton Relaxivity Measurements. The longitudinal water proton relaxation rates were measured by using a Stelar Spinmaster (Mede, Pavia, Italy) spectrometer operating at 0.47 T by means of the standard inversion−recovery technique (16 experiments, 2 scans). A typical 90° pulse width was 7.5 μs and the reproducibility of the T_1 data was ±0.5%. The temperature was controlled with a Stelar VTC-91 air-flow heater equipped with a copper-constantan thermocouple (uncertainty ± 0.1 °C). The proton $1/T_1$ NMRD profiles were measured over a continuum of magnetic field strength from 0.00024 to 0.47 T (corresponding to 0.01−20 MHz proton Larmor Frequency) on a Stelar field-cycling relaxometer. The relaxometer works under complete computer control with an absolute uncertainty in $1/T_1$ of ±1%. Data points from 0.47 T (20 MHz) to 1.7 T (70 MHz) were collected on a Stelar Spinmaster spectrometer working at variable field. The quantitative analysis of NMRD profiles has been performed by the use of an NMRD program kindly provided by CERM, University of Florence.

Cellular Uptake. Male Wistar rats weighing 150−200 g were used to isolate hepatocytes by the collagenase perfusion method.[26] Their care was in accordance with the national guidelines for animal experimentation. The cells were plated at a density of 70 000 viable cells/cm^2 on culture dishes (10 cm diameter) coated with rat tail tendon collagen prepared as described[27] in M199 medium supplemented with 2 mg/mL BSA, 3.6 mg/mL HEPES, 100 U/mL penicillin, 100 μg/mL streptomycin, 5% fetal bovine serum (FBS), and 1 nmol/L insulin and incubated in a humidified incubator with a CO_2/air atmosphere (5:95 v/v) at 37 °C. Four hours after cell seeding, the M199 medium was changed to fresh M199 supplemented with 10 nmol/L insulin instead of FBS, and the cells were incubated as described above. Cells were used for the uptake experiments after 24 h of culture. HTC (Rat Hepatoma Tissue Culture) were grown in 75 cm^2 flasks in DMEM-F12 medium supplemented with 5% FBS, 100 U/mL penicillin, and 100 μg/mL streptomycin. The cells were then seeded in culture dishes (10 cm diameter) at a density of about 25 000 cells/cm^2. After 24 h, cells were ready for the uptake experiments: the medium was removed, both rat hepatocytes and HTC were washed with 5 mL of phosphate saline buffer (PBS) and then incubated at 37 °C for 6 h with 5 mL of Earl's Balanced Salt Solution (EBSS: $CaCl_2$, 0.266 g/L; KCl, 0.4 g/L; NaCl, 6.8 g/L; glucose, 1 g/L; $MgSO_4$, 0.204 g/L; NaH_2PO_4, 0.144 g/L; $NaHCO_3$, 1.1 g/L; pH 7.4) in the presence of 0.25 mM concentration of each Gd(III) complex. Each value for the uptake experiments is the average of three experiments. At the end of the uptake experiment the medium was removed; the cells (ca. 5×10^6) were washed three times with 5 mL of ice-cold PBS and collected in 250 μL of PBS. Cells were then sonicated and treated with 250 μL of HCl 37%. Upon heating at 120 °C for 16 h in harsh acidic conditions, all Gd^{3+} is dissolved as free aquo-ion. By measuring the proton relaxation rate (R_{1obs}) at 20 MHz, 25 °C (Stelar Spinmaster, Mede, Italy) of these solutions, it is possible to determine the Gd^{3+} concentration. In fact, R_{1obs} is proportional to the concentration of the paramagnetic Gd^{3+} ion according to the formula

$$R_{1obs} = R_{1d} + [Gd^{3+}] \times r_{1p}^{Gd^{3+}}$$

where R_{1d} is the relaxation rate obtained with the same number of untreated cells, and $r_{1p}^{Gd^{3+}}$ is the millimolar relaxivity of the Gd ion (13.5 s^{-1} mM^{-1} in a 6 M HCl solution). The method has been checked out by using atomic standard solutions of Gd^{3+} ion and double-checked with parallel ICP−MS measurements. Protein concentration of each sample was determined from cell lysates by the Bradford method[28] using bovine serum albumin as standard.

NMR Spectroscopy Experiments and Data Analysis. All samples were prepared in 30 mM sodium phosphate buffer, pH 7, containing 0.03% NaN_3 and 10% D_2O unless otherwise stated. The measurements were performed with a Bruker DRX 500 spectrometer, operating at 500.13 MHz proton Larmor frequency, equipped with a triple resonance probe head, incorporating gradients in the *z*-axis. The measurement temperature was 25 °C. Pulse programs from the standard Bruker library (Topspin 1.3) were used.

The experiments for proton resonances assignment of the bile acid-derived complexes were run on 1 mM samples of compound **1**, Y-1 and Gd-1. 2D phase-sensitive TPPI−TOCSY and double quantum filtered COSY spectra were run with 32 or 64 scans and 2048 × 400 complex time domain points on a spectral window of 6510 Hz in both dimensions. The relaxation delay was set to 1.5 s and the acquisition time was 157 ms. TOCSY mixing times of 70 ms or 20 ms were used. The suppression of the water signal was achieved through excitation sculpting. The data were Fourier-transformed into a matrix of 2048 × 1024 computer points after apodization. 2D *J*-resolved correlation spectra with solvent presaturation were run with 64 scans, 8192 × 128 complex data points covering 60 Hz in the F_1 (*J*-coupling) domain. Prior to the double FT and magnitude calculation, the F_1 data were zero-filled to 1024 computer points and apodized by means of a sinebell function in F_2 and a sine-bell-squared function in F_1. The spectra were tilted by 45° to provide orthogonality of the chemical shift and coupling constant axes and subsequently symmetrized about the F_1 axis. Spectra were displayed both in the form of contour plots and as skyline F_2 projections.

The following triple resonance experiments were recorded on [^{15}N, ^{13}C]-cLBABP/Y-1: (i) HNCA [1024 (^1H) × 40 (^{15}N) × 104 (^{13}C) complex data points, 8 scans] acquired on a Bruker Avance 900 spectrometer, operating at 900.13 MHz proton Larmor frequency, equipped with a triple resonance cryoprobe, incorporating gradients in the *z*-axis; (ii) HBHA(CO)NH [2048 (^{15}N) × 40 (^{15}N) × 128 (^1H) complex data points, 64 scans] acquired at 500.13 MHz.

A STD NMR experiment[23] was performed on a solution containing 30-fold molar excess of Y-1 (1.2 mM) over the protein cL-BABP. For the acquisition, a 1D pulse sequence incorporating a $T_{1\rho}$ filter and water suppression by excitation sculpting was used. On-resonance irradiation was performed at 5.9 ppm after discarding different possibilities that caused unwanted direct saturation of ligand resonances, and off-resonance was obtained irradiating at 30 ppm. Irradiation was performed using 50 Gaussian pulses with a 1% truncation and 50 ms duration of intensity $\gamma B_1 = 129$ Hz, to give a total saturation time of 2.5 s. The duration of the $T_{1\rho}$ filter was 100 ms ($\gamma B_1 = 4965$ Hz). The STD spectrum was acquired with a total of 128 transients for 32 K data points over a spectral width of 13 ppm.

NMR titration experiments with Y-1 were run on 0.4 mM ^{15}N-enriched cL-BABP. The ligand was added stepwise from a concentrated stock in the measurement buffer and incubated for at least 30′. The following protein/ligand ratios were analyzed by

running HSQC correlation spectra (^{1}H−^{15}N-HSQC): 1:0.025, 1:0.05, 1:0.25, 1:0.5, 1:0.75, 1:1, 1:1.25, 1:2, 1:3, 1:5. A similar experimental approach was used to analyze the interaction of Gd-1 to labeled cL-BABP, at molar ratios of 1:0.05 and 1:0.1. Intensity attenuations were calculated as $(I^{dia} - I^{para})/I^{dia}$, where I^{para} was measured from the samples containing Gd-1, while I^{dia} was measured from the samples containing Y-1 in the same protein−ligand molar ratios. To evaluate the paramagnetic effect of gadolinium in saturating conditions, another set of experiments was run by adding to a protein/Y-1(1:5) sample, aliquots of a stock containing the same concentrations of protein/Gd-1(1:5). In this way, the protein and total ligand concentrations were kept fixed, while changing only the Y-1/Gd-1 molar ratio. HSQC measurements were run on samples containing BABP/Y-1/Gd-1 in molar ratios of 1:5:0 (used as diamagnetic reference to evaulate I^{dia}), 1:4.76:0.24 and 1:4.55:0.45. Finally, a competition experiment was run using a 0.4 mM unlabeled-protein sample and ^{15}N-labeled GCDA at a molar ratio of 1:0.3. The signals of the bound GCDA and the displacement of GCDA after addition of unlabeled Y-1 at a final protein/Y-1 molar ratio of 1:5 were observed via HSQC NMR spectroscopy. ^{1}H−^{15}N-HSQC spectra were collected as gradient- and sensitivity-enhanced correlation spectra and acquired with a ^{1}H spectral width of 6010 Hz and 2048 complex points, zero-filled to a total of 2048 points. In the ^{15}N dimension, 128 hypercomplex increments were collected and zero-filled to a total of 512 points. Typically 8, 16, or 32 transients were collected. In the case of the competition experiment, the number of scans was increased to 1024, and the number of collected increments decreased to 48. Spectra analysis and peak intensity measurements were performed with Topspin 1.3 (Bruker, Karlsruhe) and Sparky 3.11 (UCSF). The chemical shift changes in the titration experiment were analyzed both as separate proton and nitrogen frequencies and as weighted average displacements. The NMR isotherms were fitted to a single-step one-site binding model to obtain K_d values with the MATLAB program, according to the following equation

$$\Delta\delta_{obs} = \left(\frac{\delta_b - \delta_f}{2C_P}\right)[(C_P + C_L + K_d) - \sqrt{(C_P + C_L + K_d)^2 - 4C_P C_L}] \quad (1)$$

where δ_{obs}, δ_b, and δ_f are the chemical shifts of the protein signals in the observed, bound, and free states; C_P and C_L are the total concentrations of the protein and the ligand, respectively.

Protein stock solution concentrations were determined by UV, while the ligand stock solutions were determined by measuring dry weights using a microbalance. Random samples were prepared three times, and the error on the measured points reflects the standard deviation from the mean.

Acknowledgment. This research was supported by FIRB 2003 (Grant RBNE03B8KK) and MIUR 2004 from the Italian Ministry for Education, University and Research. The support of CIRMMP (Consorzio Interuniversitario di Risonanze Magnetiche di Metalloproteine Paramagnetiche) is gratefully acknowledged. Ivano Bertini, Claudio Luchinat, and Giacomo Parigi from CERM, University of Florence, kindly provided their software for relaxometric analysis. Lucia Zetta (ISMAC, CNR, Milano) critically read the manuscript and Mara Guariento and Massimo Pedò (University of Verona) helped in protein expression.

Supporting Information Available: Relaxometric determination of the binding affinity between Gd−L complexes and cL-BABP (PRE method). This material is available free of charge via the Internet at http://pubs.acs.org.

References

(1) Houten, S. M.; Watanabe, M.; Auwerx, J. Endocrine functions of bile acids. *EMBO J.* **2006**, *25*, 1419−25.
(2) Chiang, J. Y. Bile acid regulation of gene expression: Roles of nuclear hormone receptors. *Endocr. Rev.* **2002**, *23*, 443−63.
(3) Russell, D. W. The enzymes, regulation, and genetics of bile acid synthesis. *Annu. Rev. Biochem.* **2003**, *72*, 137−74.
(4) Qiao, L.; Han, S. I.; Fang, Y.; Park, J. S.; Gupta, S.; Gilfor, D.; Amorino, G.; Valerie, K.; Sealy, L.; Engelhardt, J. F.; Grant, S.; Hylemon, P. B.; Dent, P. Bile acid regulation of C/EBPbeta, CREB, and c-Jun function, via the extracellular signal-regulated kinase and c-Jun NH2-terminal kinase pathways, modulates the apoptotic response of hepatocytes. *Mol. Cell. Biol.* **2003**, *23*, 3052−66.
(5) Dawson, P. A.; Oelkers, P. Bile acid transporters. *Curr. Opin. Lipidol.* **1995**, *6*, 109−14.
(6) Ragona, L.; Catalano, M.; Luppi, M.; Cicero, D.; Eliseo, T.; Foote, J.; Fogolari, F.; Zetta, L.; Molinari, H. NMR dynamic studies suggest that allosteric activation regulates ligand binding in chicken liver bile acid-binding protein. *J. Biol. Chem.* **2006**, *281*, 9697−709.
(7) Nichesola, D.; Perduca, M.; Capaldi, S.; Carrizo, M. E.; Righetti, P. G.; Monaco, H. L. Crystal structure of chicken liver basic fatty acid binding protein complexed with cholic acid. *Biochemistry* **2004**, *43*, 14072−9.
(8) Tochtrop, G. P.; Richter, K.; Tang, C.; Toner, J. J.; Covey, D. F.; Cistola, D. P. Energetics by NMR: Site-specific binding in a positively cooperative system. *Proc. Natl. Acad. Sci. U.S.A.* **2002**, *99*, 1847−52.
(9) Tomaselli, S.; Ragona, L.; Zetta, L.; Assfalg, M.; Ferranti, P.; Longhi, R.; Bonvin, A. M. J. J.; Molinari, H. NMR-based modelling and binding studies of a ternary complex between chicken liver bile acid binding protein and bile acids. *Proteins* **2007**, *69*, 177−191.
(10) Anelli, P. L.; Lattuada, L.; Lorusso, V.; Lux, G.; Morisetti, A.; Morosini, P.; Serleti, M.; Uggeri, F. Conjugates of gadolinium complexes to bile acids as hepatocyte-directed contrast agents for magnetic resonance imaging. *J. Med. Chem.* **2004**, *47*, 3629−41.
(11) von Dippe, P.; Levy, D. Expression of the bile acid transport protein during liver development and in hepatoma cells. *J. Biol. Chem.* **1990**, *265*, 5942−5.
(12) Cavagna, F. M.; Lorusso, V.; Anelli, P. L.; Maggioni, F.; de Haen, C. Preclinical profile and clinical potential of gadocoletic acid trisodium salt (B22956/1), a new intravascular contrast medium for MRI. *Acad. Radiol.* **2002**, *9* (Suppl 2), S491−4.
(13) Libra, A.; Fernetti, C.; Lorusso, V.; Visigalli, M.; Anelli, P. L.; Staud, F.; Tiribelli, C.; Pascolo, L. Molecular determinants in the transport of a bile acid-derived diagnostic agent in tumoral and nontumoral cell lines of human liver. *J. Pharmacol. Exp. Ther.* **2006**, *319*, 809−17.
(14) Lorusso, V.; Pascolo, L.; Fernetti, C.; Visigalli, M.; Anelli, P.; Tiribelli, C. In vitro and in vivo hepatic transport of the magnetic resonance imaging contrast agent B22956/1: Role of MRP proteins. *Biochem. Biophys. Res. Commun.* **2002**, *293*, 100−5.
(15) Karabulut, N.; Elmas, N. Contrast agents used in MR imaging of the liver. *Diagn. Interv. Radiol.* **2006**, *12*, 22−30.
(16) De Haen, C.; Beltrami, A.; Cappelletti, E.; Lattuada, L.; Virtuani, M. Bile acid conjugates with metal ion chelates and the use thereof. U.S. Patent US2003113265.2003, 2003.
(17) Kirsch, J. E. Basic principles of magnetic resonance contrast agents. *Top. Magn. Reson. Imaging* **1991**, *3*, 1−18.
(18) Bertini, I.; Galas, O.; Luchinat, C.; Parigi, G. Computer Program for the calculation of paramagnetic enhancements nuclear-relaxation rates in slowly rotating systems. *J. Magn. Reson.* **1995**, *113*, 151−156.
(19) Bertini, I.; Kowalewski, J.; Luchinat, C.; Parigi, G. Cross correlation between the dipole-dipole interaction and the Curie spin relaxation: The effect of anisotropic magnetic susceptibility. *J. Magn. Reson.* **2001**, *152*, 103−8.
(20) Aime, S.; Chiaussa, M.; Digilio, G.; Gianolio, E.; Terreno, E. Contrast agents for magnetic resonance angiographic applications: H-1 and O-17 NMR relaxometric investigations on two gadolinium(III) DTPA-like chelates endowed with high binding affinity to human serum albumin. *J. Biol. Inorg. Chem.* **1999**, *4*, 766−774.
(21) Aime, S.; Gianolio, E.; Longo, D.; Pagliarin, R.; Lovazzano, C.; Sisti, M. New insights for pursuing high relaxivity MRI agents from modelling the binding interaction of Gd-III chelates to HSA. *ChemBioChem* **2005**, *6*, 818.
(22) Waterhous, D. V.; Barnes, S.; Muccio, D. D. Nuclear magnetic resonance spectroscopy of bile acids. Development of two-dimensional NMR methods for the elucidation of proton resonance assignments for five common hydroxylated bile acids, and their parent bile acid, 5 beta-cholanoic acid. *J. Lipid Res.* **1985**, *26*, 1068−78.
(23) Meyer, B.; Peters, T. NMR spectroscopy techniques for screening and identifying ligand binding to protein receptors. *Angew. Chem., Int. Ed.* **2003**, *42*, 864−90.
(24) Shuker, S. B.; Hajduk, P. J.; Meadows, R. P.; Fesik, S. W. Discovering high-affinity ligands for proteins: SAR by NMR. *Science* **1996**, *274*, 1531−4.

(25) Vasile, F.; Ragona, L.; Catalano, M.; Zetta, L.; Perduca, M.; Monaco, H.; Molinari, H. Solution structure of chicken liver basic fatty acid binding protein. *J. Biomol. NMR* **2003**, *25*, 157−60.
(26) Probst, I.; Unthan-Fechner, K. Activation of glycolysis by insulin with a sequential increase of the 6-phosphofructo-2-kinase activity, fructose-2,6-bisphosphate level and pyruvate kinase activity in cultured rat hepatocytes. *Eur. J. Biochem.* **1985**, *153*, 347−353.
(27) Strom, C. S.; Michalopoulos, G. Collagen as substrate for cell growth and differentiation. *Methods Enzymol.* **1982**, *82*, 544−555.
(28) Bradford, M. M. A rapid and sensitive method for the quantitation of microgram quantities of protein utilizing the principle of protein−dye binding. *Anal. Biochem.* **1986**, *72*, 248−254.

JM070397I